

Single-band model for the temperature-dependent Hall coefficient of high- T_c superconductors

Chris Kendziora, David Mandrus, and Laszlo Mihaly

Department of Physics, State University of New York, Stony Brook, New York 11794-3800

Laszlo Forro*

Department of Physics, Ecole Polytechnique Federale de Lausanne, 1015 Lausanne, Switzerland

(Received 26 August 1992)

We have studied the resistivity ρ and the Hall constant R_H on a series of compounds derived from $\text{Bi}_2\text{Sr}_2\text{Ca}_1\text{Cu}_2\text{O}_8$ by oxygen treatment, Y, Ni, and Zn doping. We observe approximately quadratic temperature dependence for the Hall angle as long as the resistivity is linear. We interpret the results in terms of a one-band Fermi-liquid model.

The Hall coefficient R_H of the high-temperature superconductors is strongly temperature dependent. A universal, approximately T^{-1} behavior has been seen for $\text{YBa}_2\text{Cu}_3\text{O}_7$,¹ $\text{Bi}_2\text{Sr}_2\text{CaCu}_2\text{O}_8$,² and $\text{La}_{2-x}\text{Sr}_x\text{CuO}_4$.³ Compounds with similar structure but no superconductivity [like the metallic $\text{Bi}_2\text{Sr}_2\text{CuO}_6$,⁴ or the semiconducting yttrium-doped material $\text{Bi}_2\text{Sr}_2\text{Ca}_{1-x}\text{Y}_x\text{Cu}_2\text{O}_8$ (Ref. 5)] have a roughly temperature-independent R_H . Therefore it has been hypothesized that the characteristic temperature dependence of the Hall coefficient, together with the approximately linear resistivity $\rho(T)$ curve is somehow related to the superconductivity in these materials.

In the Fermi-liquid picture the combination of anisotropic scattering and interesting Fermi-surface topology permits a temperature dependent R_H ,⁶ and this is often seen in systems as simple as aluminum. However, a universal behavior, as observed in the high- T_c materials, is hard to explain in conventional transport theory. The most common approaches are based on a two band model, where a near perfect cancellation of the first-order contributions from the “electronic” and “hole” bands is required. It is unlikely that this cancellation could occur systematically over such a wide range of materials or be independent of pressure.⁷ Anderson⁸ argued that this behavior cannot be understood in the framework of conventional Fermi-liquid theory, and he interpreted the experiments in terms of spinon-spinon scattering.

Ong and co-workers^{7,9} established that the Hall angle, $\tan\Theta_H = R_H = R_H H / \rho$ exhibits T^{-2} dependence and that the Hall conductivity $\sigma_H = R_H H / \rho^2$ exhibits T^{-3} (Ref. 10) behavior, even in samples with higher impurity concentrations and reduced carrier densities, for which R_H and ρ do not have simple T dependencies. Carrington *et al.* have shown that superconducting cobalt-doped $\text{YBa}_2\text{Cu}_3\text{O}_7$ crystals, with unusual curvature in ρ and R_H , still give a good T^2 dependence of the Hall angle.¹¹ In this work we report further results on four sets of samples, obtained by modifying $\text{Bi}_2\text{Sr}_2\text{Ca}_1\text{Cu}_2\text{O}_8$ in different ways: (1) heat treatment in reduced oxygen pressure, (2) yttrium, (3) nickel, and (4) zinc doping. Each series of samples provides unique insight into the mechanism of conduction in $\text{Bi}_2\text{Sr}_2\text{Ca}_1\text{Cu}_2\text{O}_8$. Removal of oxygen, as

well as Y doping, changes the carrier density and increases impurity scattering. Ni and Zn are expected to replace Cu, introducing scattering centers in the conducting CuO plane. Susceptibility measurements by Maeda *et al.*¹² show that, in contrast to Zn, Ni is magnetic in these compounds. For each set of samples we measured the resistivity and the Hall coefficient for temperatures from 300 K down to T_c (or 4.2 K) for nonsuperconducting samples). We provide a simple interpretation for the results in terms of a single-band, conventional Fermi-liquid picture.

Single-crystals were grown from a copper-oxide-rich melt as described in detail elsewhere.¹³ The oxygen deficiency of the samples is characterized by the oxygen pressure during the heat treatment; the procedure is described in Ref. 14. For the yttrium- and nickel-doped samples, we report the composition as measured on the crystals by electron probe analysis. For zinc doping microprobe measurements were not performed; the nominal composition was 10% zinc relative to copper.

The crystals were cut into rectangular shape of typical dimensions $1 \text{ mm} \times 1 \text{ mm} \times 5 \text{ } \mu\text{m}$ with the shortest dimension lying along the c axis. The size of each sample was measured using the calibrated eyepiece of a high-power optical microscope. The thickness measurement is the least accurate ($\sim 10\%$). This may influence the absolute values of resistivity and Hall coefficient, but cancels in the Hall angle. Six electrical contacts were fired onto the samples; two “line” contacts running along opposite edges and four “point” contacts, two on each remaining edge. Resistances were $\sim 1 \Omega$ for both kinds of contacts. With this configuration, simultaneous four-probe measurements could be taken of the Hall voltage and resistance. The Hall measurements were made in a 7-T magnetic field with current densities of $\sim 10^2 \text{ A/cm}^2$. To reduce systematic errors the current polarity was reversed and the sample was rotated by 180° with respect to the magnetic field. For temperatures above 100 K, the Hall voltage was linear with both field and current up to the highest values used—8 T and $1 \times 10^3 \text{ A/cm}^2$.

In Figs. 1 and 2 we show the resistivity and Hall coefficient for representative samples of each set. Note that oxygen deficiency and yttrium doping lead to a pro-

nounced increase of the Hall coefficient and to an upturn of the low-temperature resistivity. Qualitatively, this can be understood as a consequence of the reduced carrier density and electron localization at low temperatures. The Ni and Zn doping do not change the Hall effect dramatically, but the resistivity is shifted to higher values, indicating extra impurity scattering. Attempts to increase Ni and Zn content further resulted in multiphase samples of drastically different chemical compositions.

In Fig. 3 the cotangent of the Hall angle, calculated from the resistivity and Hall coefficient, is plotted. Note that increased resistivity and increased Hall coefficient lead to rather similar Hall angles.

As a starting point for the interpretation, we use Ong's results on the transport properties of the two-dimensional electron gas.¹⁵ The electron transport is treated in the Boltzmann equation, and the scattering is represented by a scattering time τ_k , depending on the electron wave number k . The conductivity $\sigma = 1/\rho$ is expressed as

$$\sigma = e^2 / (2\pi\hbar) \int ds l, \quad (1)$$

where $\hbar/e^2 = 26 \text{ k}\Omega$, the integration is over the Fermi surface (Fermi "line" in two dimensions), and

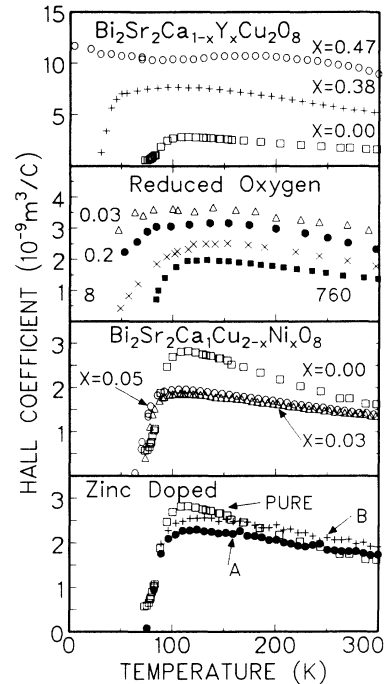


FIG. 2. Hall coefficient R_H , as a function of temperature, for the samples identical to those in Fig. 1. The apparent reversal of the magnitude of Hall coefficients of the $x = 0.03$ and 0.05 samples is probably due to the inaccuracy of thickness measurement.

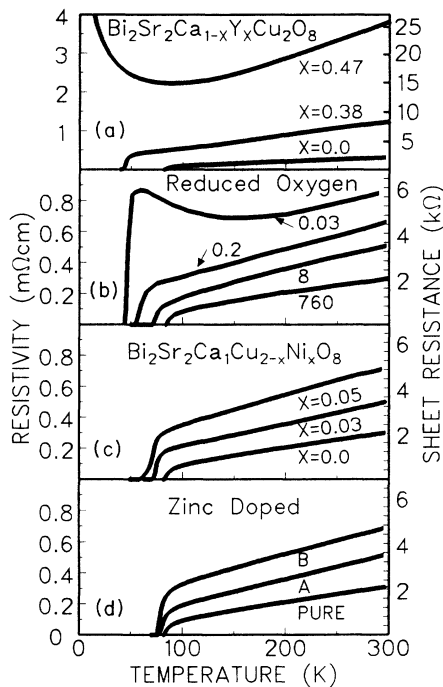


FIG. 1. Resistivity as a function of temperature for four sets of $\text{Bi}_2\text{Sr}_2\text{Ca}_1\text{Cu}_2\text{O}_8$ single crystals with different dopants. The right axis of each panel rescales the resistivity into sheet resistance as defined by $\rho_{\text{sheet}} = \rho_{\text{measured}}/d$ where $d = 15 \text{ \AA}$ is the distance between CuO planes. Panel (a) shows samples where yttrium has partially replaced calcium by the amount x . For panel (b), samples were annealed in various partial pressures of oxygen; the numbers belonging to the various symbols indicate oxygen pressure in mm of Hg. Panel (c) shows the data for crystals in which nickel has replaced copper by the amount x . Panel (d) displays data for samples in which zinc has partially replaced copper. The two Zn-doped samples, denoted by A and B , had the same nominal 10% Zn composition.

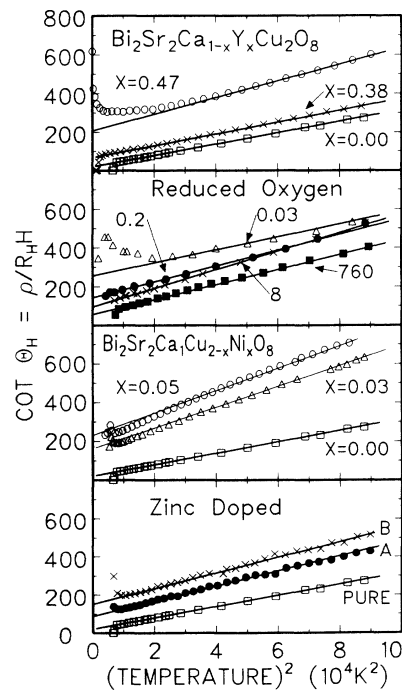


FIG. 3. The cotangent of the Hall angle, defined as $\rho/R_H H$, is plotted as a function of temperature squared for the four doped series. The data are generated from Figs. 1 and 2 using the magnetic field of 7 T. The lines are drawn as guides to the eye and suggest linearity in T^2 for the $\text{cot}\theta_H$. Note that all data are plotted on the same scale.

$l = |\mathbf{v}_F(\mathbf{k})\tau_{\mathbf{k}}|$ is the mean free path. The Hall conductivity is

$$\sigma_H = (e^2/h)HA/\Phi_0, \quad (2)$$

where $\Phi_0 = h/2e = 2.07 \times 10^{-7}$ Gauss cm² is the flux quantum, H is the magnetic field, and A is an area scanned by the $\mathbf{v}_F(\mathbf{k})\tau_{\mathbf{k}}$ vectors as \mathbf{k} varies along the Fermi surface.

In Fig. 4 we illustrate the construction of area A for a nearly half-filled tight binding band and isotropic relaxation rate τ . For the “straight” segments of the Fermi surface $\mathbf{v}_F = \mathbf{v}_1$ is relatively large, and its x and y components are approximately equal; the corresponding mean free path is l_1 . For the “corners” the Fermi velocity is small, and the direction scans over a wider range of angles. The shortest mean free path is $l_2 = v_2\tau$. The corresponding points in the $\mathbf{v}_F\tau$ plot make a four pointed star; the area of this star is approximately $4\sqrt{2}l_1l_2$. The closer the band is to being half filled, the longer the points of the star will be.

The key to the interpretation of the experimental results is that the conductivity, Eq. (1), and the Hall conductivity, Eq. (2), have fundamentally different dependencies on the parameters l_1 and l_2 . The conductivity is derived as a weighted *average* of large and small l values; it is dominated by the large ones:

$$\sigma \approx (e^2/h)(2\sqrt{2}/\pi)k_F v_1 \tau_1 \sim l_1. \quad (3)$$

Here $k_F \approx \pi/a$, where a is the lattice spacing. The relevant integration length is estimated to be $4\sqrt{2}k_F$. On the other hand, the Hall conductivity depends on the product of the large and small numbers

$$\sigma_H \approx (e^2/h)(H/\Phi_0)4\sqrt{2}v_1v_2\tau_1\tau_2 \sim l_1l_2. \quad (4)$$

In our approximate treatment the Hall angle depends on the short l alone,

$$\tan\Theta_H = \sigma_H/\sigma \approx 2\pi/k_F(H/\Phi_0)v_2\tau \sim l_2. \quad (5)$$

We represent the temperature dependence of the relaxation rate by $1/\tau_{\mathbf{k}} = AT^2 + BT + C$. One may either view this expression as a Taylor expansion, or attribute specific processes to the various terms, as we will later attempt to do. For isotropic $\tau_{\mathbf{k}}$ the Hall coefficient is independent of temperature.¹⁵ To obtain the required temperature dependence we postulate that the coefficients A , B , and C , depend on \mathbf{k} , and in such a way that for high Fermi

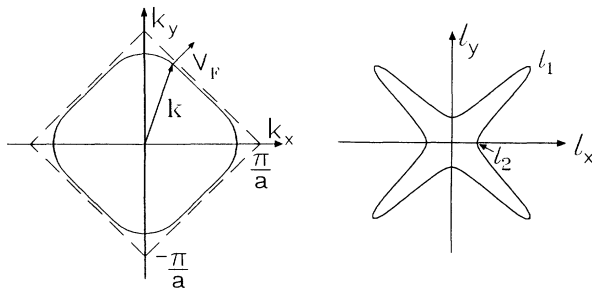


FIG. 4. Schematic representation of the Fermi surface and the l (mean free path) curve for a nearly half-filled band.

velocities the BT then dominates while for low Fermi velocities the AT^2 term dominates. Therefore $l_1 = v_1\tau_1 = v_1/BT$ and $l_2 = v_2\tau_2 = v_2/AT^2$. As long as $l_1 \gg l_2$ the conclusions of the previous paragraph prevail, but l_1 and l_2 will have different temperature dependencies. Consequently, from Eqs. (3)–(5) we obtain $\sigma \sim 1/T$, $\tan\Theta_H \sim 1/T^2$, and $\sigma_H \sim 1/T^3$. The Hall coefficient will show $R_H \sim 1/T$.

The various terms in the temperature dependence of the relaxation rates can be tentatively identified as follows. The constant term is due to impurities, and it is expected to be isotropic. The quadratic temperature dependence most likely arises from electron-electron scattering; in our case this term may be important for the parts of the Fermi surface with *low* Fermi velocity. The linear term may be due to electron-phonon interactions as long as the temperature is not much smaller than the Debye temperature. Alternatively, or parallel to the phonon processes, electron-electron scattering may lead to a linear temperature dependence of $1/\tau$ for the “nested” (i.e., *high* Fermi velocity) parts of the Fermi surface, as suggested by Virosztek and Ruvalds.¹⁶ The anisotropy in the temperature dependence of the relaxation rate naturally follows from the nested Fermi-liquid picture, since the “corners” of the Fermi surface are not nested, and no linear contribution is expected in the temperature range studied here.

To make more specific numerical comparison to the data, we rescale the experimental resistivities to the sheet resistance (Fig. 1, right-hand scale). We will consider the CuO double layers, separated by a distance of $d = 15$ Å, to be quasi-two-dimensional; therefore, the sheet conductivity is related to the measured conductivity by $\sigma = \sigma_{\text{meas}}d$. A typical mean free path evaluated from the conductivity of $(100 \mu\Omega \text{ cm})^{-1}$ is $v_1\tau_1 = (\sigma_{\text{meas}}dah)/(1\sqrt{2}e^2) = 14a$, a reasonable number for Boltzmann transport. From Eq. (5), and from the measured Hall angles ($\cot\Theta_H = 100$) we can obtain an estimate for the shorter mean free path: $v_2\tau_2 = k_F/\pi \tan\Theta_H(\Phi_0/H) = 5.4a$.

For the doped samples we see a significant deviation from the “ideal,” power-law temperature dependence of R_H and σ_H , while the $\rho(T)$ and $\cot\Theta_H$ vs T^2 still make reasonably straight lines. Impurity scattering (the constant term C in the relaxation rate) offers a possible explanation of this phenomenon: a temperature-independent term in the relaxation rate leads to a *shift* of the $\rho(T)$ and $\cot\Theta_H(T)$ curves, while R_H and σ_H are influenced in a more complicated way. If impurity scattering dominates both τ_1 and τ_2 , the Hall coefficient is expected to saturate at the temperature-independent value of $R_H = \pi^2/(\sqrt{2}e)k_F^{-2}(v_2/v_1)$. Saturation is clearly observed around 100 K for the Y- and O₂-doped samples. The present interpretation is unable to deal with the low-temperature upturn of resistivity in highly doped samples; we believe it is due to electron localization.⁵

In conclusion, we have presented experimental results for the Hall coefficient and resistivity of a family of high- T_c superconductors and discussed the results in terms of a single-band Fermi-liquid model with anisotropic relaxation rates. In this model the Hall angle and the resistivity

have simple relationships to the mean free path at different parts of the Fermi surface. Although we used a nearly half-filled tight binding band to illustrate our point, the interpretation does not rely exclusively on this band structure. The model may have observable consequences on other experiments, like Raman scattering, which are sensitive to anisotropic electron relaxation.

The work at Stony Brook has been supported by the NSF Grant No DMR 901-6456 and in Lausanne by Swiss National Foundation Grant No. 4030-032779. We are grateful to John Cooper for participating in the measurements of the oxygen-coped samples and for pointing out the possibility of single-band interpretation of the Hall data.

*Permanent address: Institute of Physics of the University, 41001 Zagreb, Croatia.

¹S. W. Cheong *et al.*, Phys. Rev. B **36**, 3913 (1987); Z. Z. Wang *et al.*, *ibid.* **36**, 7222 (1987); P. Chaudari *et al.*, *ibid.* **36**, 8903 (1987); T. Penney *et al.*, *ibid.* **38**, 2918 (1988).

²N. P. Ong, in *Physical Properties of High Temperature Superconductors*, edited by D. M. Ginsberg (World Scientific, Singapore, 1990), Vol. 2, p. 459.

³M. Suzuki *et al.*, Phys. Rev. B **39**, 2312 (1989).

⁴L. Forro, D. Mandrus, C. Kendziora, L. Mihaly, and R. Reeder, Phys. Rev. B **42**, 8704 (1990).

⁵D. Mandrus, L. Forro, C. Kendziora, and L. Mihaly, Phys. Rev. B **44**, 2418 (1991); D. Mandrus, L. Forro, C. Kendziora, and L. Mihaly, Phys. Rev. B **45**, 12 640 (1992).

⁶W. Schulz, L. Forro, C. Kendziora, R. Wentzcovitch, D. Mandrus, L. Mihaly, and P. B. Allen, this issue, Phys. Rev. B **46**, 14 001 (1992).

⁷T. R. Chien, Z. Z. Wang, and N. P. Ong, Phys. Rev. Lett. **67**, 2088 (1991); I. D. Parker and R. H. Friend, J. Phys. C **21**, L345 (1988).

⁸P. W. Anderson, Phys. Rev. Lett. **67**, 2092 (1991).

⁹T. R. Chien *et al.*, Phys. Rev. B **43**, 6242 (1991).

¹⁰Strictly speaking the Hall conductivity contains a $1 + \tan^2 \Theta_H$ factor, but for practical purposes this factor is unity.

¹¹A. Carrington, A. P. Mackenzie, C. T. Lin, and J. R. Cooper (unpublished).

¹²A. Maeda *et al.*, Phys. Rev. B **41**, 4112 (1990).

¹³C. Kendziora *et al.*, Phys. Rev. B **45**, 13 025 (1992); L. Forro, D. Mandrus, B. Keszei, L. Mihaly, and R. Reeder, J. Appl. Phys. **68**, (9), 4876 (1990).

¹⁴L. Forro, J. Cooper, B. Leontich, and B. Keszei, Europhys. Lett. **10**, 371 (1989).

¹⁵N. P. Ong, Phys. Rev. B **43**, 193 (1991).

¹⁶A. Virosztek and J. Ruvalds, Phys. Rev. B **42**, 4064 (1990).